



Comparing the adhesion strength of 316L stainless steel joints after laser surface texturing by CO₂ and fiber lasers

Chiara Mandolino¹ · Muhannad Obeidi² · Enrico Lertora¹ · Dermot Brabazon²

Received: 11 March 2020 / Accepted: 15 June 2020 / Published online: 11 July 2020
© Springer-Verlag London Ltd., part of Springer Nature 2020

Abstract

This paper focuses on the effects of the laser surface texturing process and joint configuration of stainless steel adherends on the adhesive tensile bond strength. Two different sources, a CO₂ and a fiber laser, were used and compared. In particular, proper choice of laser parameters was explored with the aim of producing different roughness and peak-to-valley distance and different textures on the bonding area, which could increase the real contact surface. Furthermore, to more thoroughly understand the effect of the laser parameters on joint fracture load, the experimental campaign was conducted according to a Design of Experiment (DoE) framework and the results were analyzed with this methodology. The creation of particular textures and roughness levels were related to the resulting joint geometrical configuration and bond strengths. In particular, significant increases in joint bond strength were achieved using both laser sources. Furthermore, by optimizing the laser parameters, smaller laser spot scan path overlaps can be achieved as well as a more refined scale of surface texture and surface roughness. This thereby enables the joining of thinner sections of different materials.

Keywords Fiber laser · CO₂ laser · Stainless steel · Adhesive bonding · Surface texture · Laser surface roughening · Statistical analysis

Nomenclature

RT	Room temperature
DoE	Design of experiment
JBS	Joint bond strength
R _a	Arithmetic mean height of the surface profile
RSM	Response surface methodology
SLJ	Single lap joint
TSS	Tensile shear strength

1 Introduction

The opportunity to change and tailor the surface characteristics of materials through “green” technologies have been

explored in recent years, especially by those interested in structural applications. Laser technologies, in particular, have several advantages, which make them suitable for surface modification. First of all, they are easily adaptable to all types of substrates, from metals to polymers, passing through composite materials, thanks to the possibility of providing high levels of concentrated energy, together with high processing speed, and thus of creating a minimal interaction time.

Processes involving the modification of the surface have the aim of creating different microstructures, making them suitable for coatings or generating structures at the microscopic and nanoscopic level to adapt them as much as possible to specific purposes.

In particular, the interaction between laser and surface layer has been exploited for various uses and successful applications of laser surface processing have been developed. For instance, localized heat treatment and surface structuring to improve wear, corrosion, and oxidation resistance have been implemented for many metallic alloys, such as steel, aluminum, magnesium, and titanium.

Surface treatment is a process that is closely related to the field of structural bonding. Indeed, the correct preparation of an adhesive bonded joint requires a superficial cleaning for the

✉ Chiara Mandolino
chiara.mandolino@unige.it

¹ Department of Mechanical Engineering, University of Genoa, Via All'Opera Pia 15, 16145 Genoa, Italy

² I-Form, and Advanced Processing Technology Research Centre, School of Mechanical & Manufacturing Engineering, Dublin City University, Dublin 9, Ireland

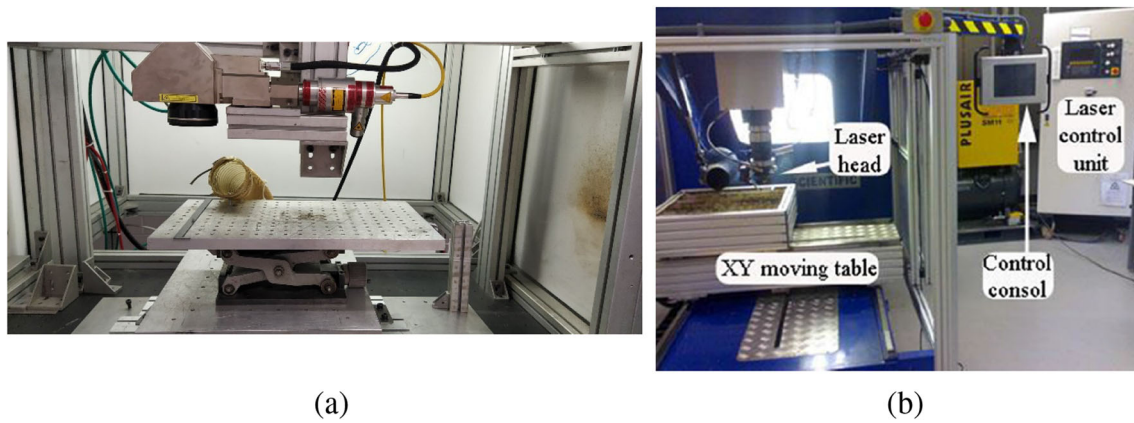


Fig. 1 Laser sources: fiber laser (a) and CO₂ laser (b)

removal of dirt and oils that could compromise the generation of adhesive bonds. If the goal is to achieve structural joints, it is necessary to plan a further surface treatment, with the aim of generating a certain surface roughness and promoting mechanical interlocking, increasing wettability, or activating the surface by creating functional groups that can chemically interact with the adhesive [1].

Traditional treatments involve the use of mechanical abrasion or chemical treatment [2–4].

Physical surface treatment processes, such as plasma [5, 6] or laser treatments [7], are promising alternatives to the abovementioned methods. The main advantages of the laser process compared to chemical or abrasion treatment are its ability to modify morphology and wettability with green technology. In fact, especially in case of metals, chemical pre-treatments are usually identified as the most effective way to increase adhesive properties, as also reported by standards [8].

Furthermore, laser preparation is not always cheaper than other treatments but is of course easily automatable, especially compared to traditional mechanical abrasion. Focusing on metallic substrates, many studies relate to the modification of titanium and aluminum alloys [9–18], as they are traditionally processed with chemical surface modification treatments. The results have mainly been positive. For example, Loutas et al. [12] performed an optimization of the laser surface treatment with the aim of improving the mechanical performance of AA2024 adhesively bonded joints. A strong increase of surface wettability was detected, in contrast to a traditional mechanical abrasion and/or acetone cleaning. Peel tests highlight that laser treatment leads to superior adhesion compared to

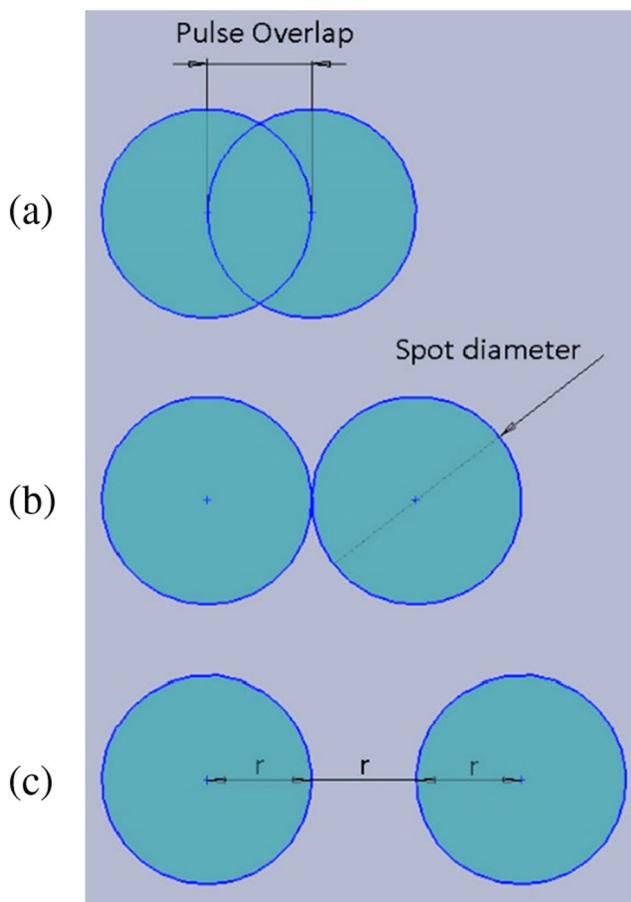


Fig. 2 Scheme of the laser texturing pattern, describing the spot overlap of **a** 50%, **b** 0%, and **c** – 50%

Table 1 Laser system characteristics

Characteristics	Symbol/value		Unit
	Fiber laser	CO ₂ laser	
Wavelength λ	1.064	10.6	μm
Operating mode	Pulsed/CW	Continuous wave	
Max. peak power	4.5	1.5	kW
Power regulation	10–100	10–100	%
Max. pulse energy	45	–	J
Pulse duration	0.05 ÷ 50	–	ms
Beam focal diameter	0.21	0.53	mm
Beam quality	TEM00	TEM00	

Table 2 Control factors and levels for laser treatments

Control factors	Labels	Low	Middle	High	Unit
Power CO ₂	PC	300	400	500	W
Power fiber	PF	450	500	550	W
Pulse percentage overlap	OL	– 50	0	50	%
Joint overlap	JO	5	10	15	mm
Response factor:	Joint bond strength (JBS)				

mechanical abrasion and/or acetone cleaning, but not similar in all cases. A Design of Experiment (DoE) approach was used to understand the effect of process parameter combination on contact angle and peel strength results.

Long-term performance of the bonded joints could also be improved, as stated by Musiari et al. [14]. They focused on the durability of the mechanical properties of aluminum joints laser pre-treated with several representative set-up parameters. These settings were also considered with the aim of proving their suitability, varying the type of stress and environmental condition, using different tests, i.e., fatigue tests and quasi-static tests after aging cycles. An interesting comparison between various surface pre-treatments for aluminum adherends was made by Rechner et al. [15], who studied in depth the interaction between laser irradiation and material surface, by comparing the laser texturing of AW6016 aluminum alloy to create bonded joints, with other surface pre-treatment techniques. An improvement in the shear strength after an accelerated aging was also observed.

An experimental campaign to study the effect of laser ablation on the performance of adhesive-bonded AA6022-T4 joints was carried out by Wu et al. [17]. An improvement in joint strength was found, probably due to an increase in surface roughness and the formation of a more uniform and thicker aluminum oxide.

Similar results were obtained on adhesive bond strength of titanium alloys, for which the effectiveness of laser ablation treatment was compared to traditional chemical surface

treatment [10, 18]. For example, Rotella et al. [18] found that laser treatment increased surface roughness and, consequently, improved joint strength, by creating a nano-patterning over the entire sample surface. Beneficial effects could also be seen after aging in boiling water. Rotella et al. in another work [19] reported the effect of pulsed laser irradiation on the strength of adhesive joints with dual phase DP500 and stainless steel AISI304 substrates. The results were compared with pre-treated samples using traditional processes of degreasing and sand blasting. In order to create useful modifications of surface morphology, a specific level of pulse fluence has to be achieved; the mechanism is to create material melting and re-solidification to generate micro roughness and increase the real contact area, exploitable for bonding. In this case, laser treatment also effectively improves static strength of the joints.

To the authors' knowledge no studies report a comparison between the effects of different laser sources and few studies have focused on stainless steel substrates. The source particularly affects the interaction between the beam and the substrate surface and the possibility of creating a surface texturing that is suitable for the penetration of the adhesive.

Indeed, increasing the contact surface and mechanical interlocking increases the mechanical resistance of adhesive bonded joints; thus, a well-executed treatment allows a proper design of the overlap between the edges to be bonded. This can be very beneficial to overcome many geometrical issues and is more suitable in many applications.

Fig. 3 Surface characterization equipment used: (a) Bruker Contour GT and (b) 3D optical microscope

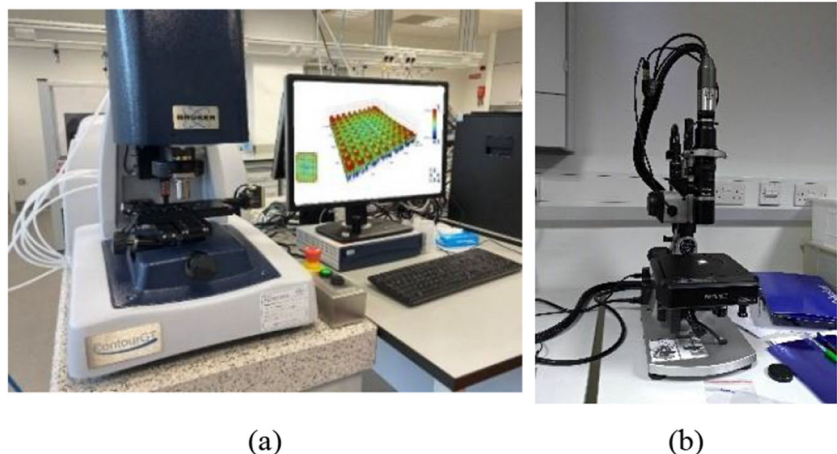
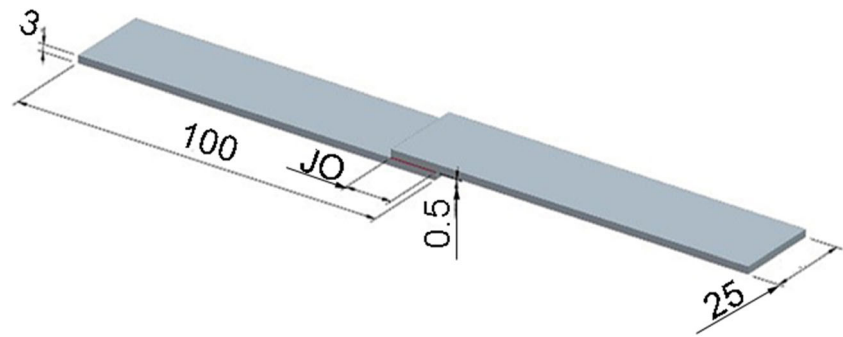


Fig. 4 Adhesive bonded joint geometry and dimensions (mm)



To summarize, the objectives of this study were mainly to

- compare the effect of two different types of laser sources on the surface roughness of stainless steel substrates;
- use the RSM to correlate the different parameters and obtain the optimal set-up;
- define the correct overlap value to obtain a certain mechanical strength, for a given set-up of parameters, using a predictive model.

2 Material and methods

2.1 Materials and surface texturing

In this study, the performance of stainless-steel homogeneous joints was investigated by employing 316L flat sheet cut into 100 mm × 25 mm × 3 mm samples. The adhesive bonding is realized using a commercial epoxy adhesive, DP490 produced by 3M™. This is a two-component thixotropic epoxy adhesive designed to be used in components requiring toughness and high mechanical strength and thus is suitable for many in-service applications, thanks also to its excellent thermal and environmental resistance. All joints were tested after a complete curing of 7 days at RT.

The surface modification of adherends was performed using two different laser sources. All the equipment is shown in Fig. 1.

Figure 2 shows the scheme of the texturing pattern, for both laser sources.

The first set of textured samples was made by using a computerized numerical controlled (CNC) CO₂ laser machine Rofin DC-015 of 1.5 kW maximum average power, and a laser beam focus diameter of 0.2 mm, positioned 1 mm below the sample surface. The other source was a YLM-450/4500-QCW multi-mode Ytterbium fiber laser by IPG. The equipment can generate a maximum average laser power of 450 W and a focus diameter of 0.53 mm. Table 1 shows the detailed characteristics of the two laser sources.

Different values of laser power and spot diameters were employed for the two sources, to take into account both the constructive difference between the machines and the different absorption ratio between the beam and the material. Stainless steel is reported to exhibit 2.5% absorption to CO₂ laser irradiation and is nearly ten times higher for the fiber laser wavelength [20].

The expected effect was a strong material ablation, in order to increase the number of microscale asperities responsible for contributing significantly to the mechanical interlocking phenomena at the interface between the adherend and the adhesive.

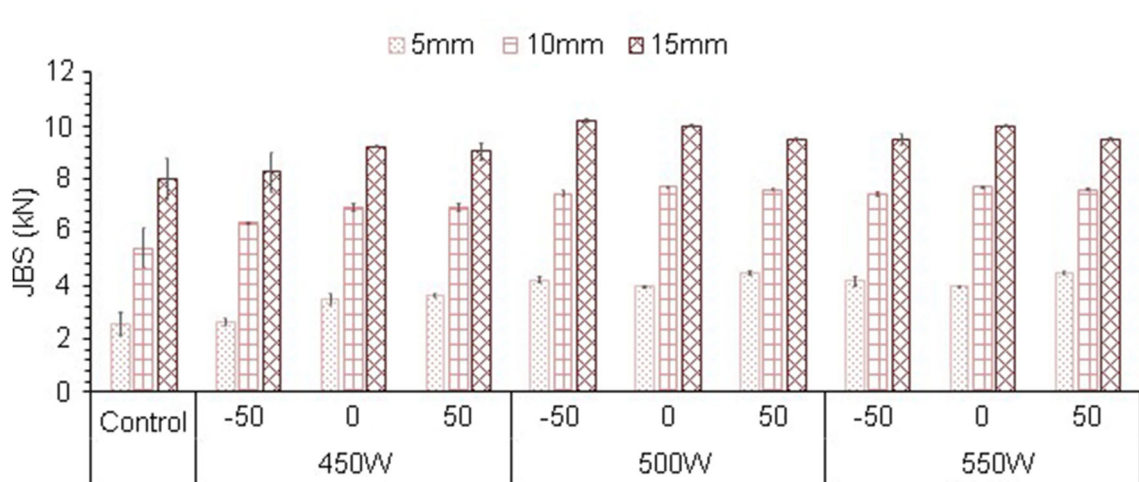


Fig. 5 JBS of adhesive bonded joints prepared with a fiber laser pre-treatment

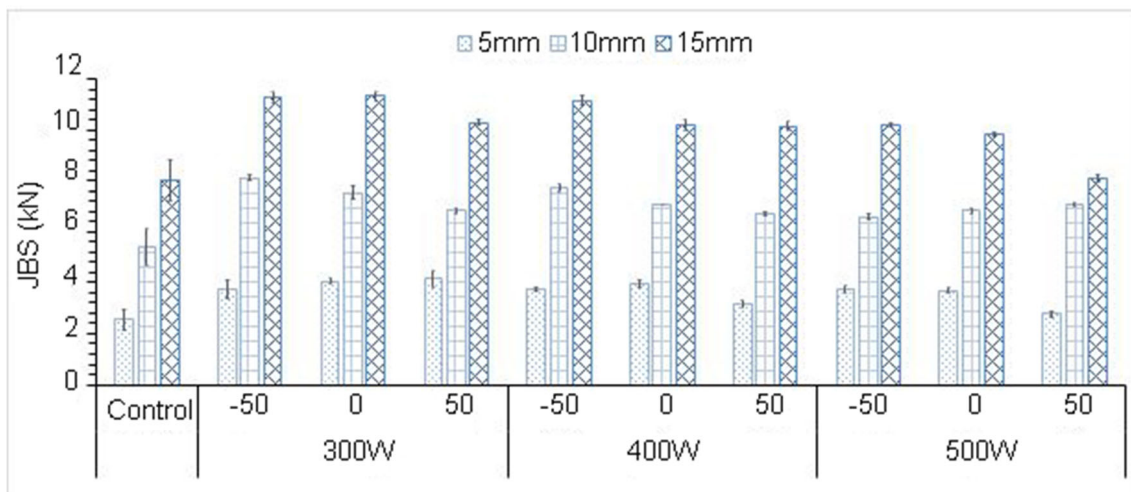


Fig. 6 JBS of adhesive bonded joints prepared with a CO₂ laser pre-treatment

2.2 Experimental design

A full factorial 3³ DoE model was designed based on preliminary test results in which the laser power, pulse percentage overlap, and the adhered joint overlap were used as the processing parameters for the estimation and optimization of the process. The aim was always the increase of the resulting surface roughness and the specific surface area of the textured surface. Table 2 lists the applied processing parameters and their level of significance. The effect of CO₂ on the surface characteristics of stainless steel was studied by some of the authors in previous works [20, 21] and provided a starting point for the choice of laser control factors and levels adopted. The fiber laser parameters were chosen in order to obtain an effect on the material comparable to the CO₂, in terms of sheet deformation.

Design-Expert 11, a dedicated software, was used to build the design matrix consisting of a set of treatment and

realization parameters using response surface methodology (RSM). The response factor was the TSS.

For result repeatability assurance, three replicates of each sample were carried out. The average value with their 95% CI was employed in the DoE model.

2.2.1 Surface characterization

The produced sample surface roughness was measured by using a non-contact surface profilometer from Bruker Contour GT and a 3D optical microscope from Keyence 2000 (Fig. 3). The modified surface roughness was characterized within an area of 5 × 5 mm with a Bruker profilometer and a 6-mm measured length on the optical microscope. The R_a of the profiles were directly calculated by the related software, following ISO 4287 standard [22].

2.3 Bonded-joint realization and quasi-static lap shear tests

The influence of laser surface treatments together with joint overlap was investigated realizing single lap joints. The epoxy adhesive was applied to the bond area of both substrates to be joined. Any excess of adhesive at the interface was expelled by pressing the joint and then removed. The reference for the geometry was ASTM D1002 [23].

The bond line thickness was kept fixed at 0.5 mm. In Fig. 4, an image of the specimen is shown. As suggested by adhesive data sheet, the assembled joints were left for 1 day at room temperature and then cured for 1 h at 80 °C before performing the mechanical tests.

For each set of laser treatment conditions and overlap shown in Table 1, three SLJs were made, tested at a test speed of 1.3 mm/min, and the mean value is reported in the results together with the related value of standard deviation.

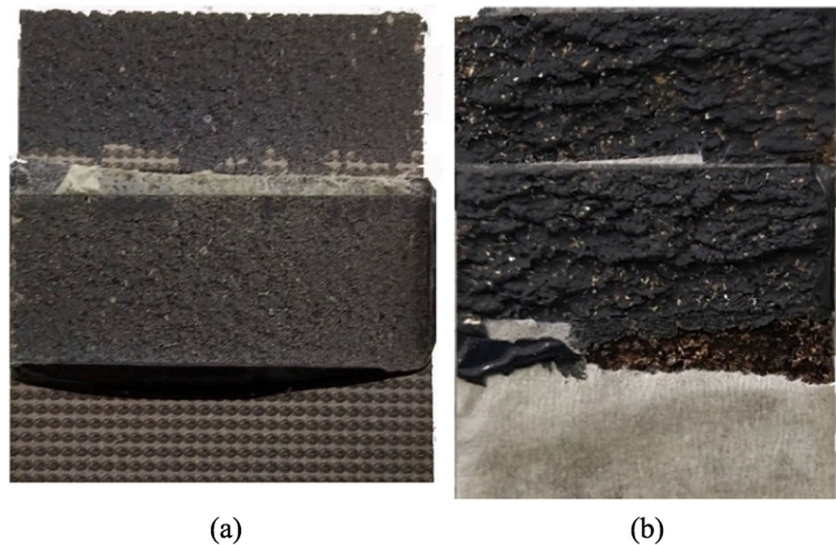
Table 3 Percentage of JBS increase of the laser treated samples

Fiber laser	Percentage of increase in JBS (%)								
	450 W			500 W			550 W		
	-50	0	50	-50	0	50	-50	0	50
5 mm	3	36	42	65	55	76	63	55	76
10 mm	18	29	28	38	43	41	38	43	41
15 mm	3	15	13	27	25	18	18	25	18

CO ₂ laser	Percentage of increase in JBS								
	300 W			400 W			500 W		
	-50	0	50	-50	0	50	-50	0	50
5 mm	46	59	63	47	55	24	47	45	9
10 mm	51	40	27	43	31	25	22	27	31
15 mm	41	42	29	39	27	27	27	23	1

In italic the pulse percentage overlap OL (%)

Fig. 7 Fracture surfaces of a fiber laser treated sample (a) and CO₂ treated sample (b)



In order to discriminate the treatment effect, the tensile shear stress (TSS), calculated as the ratio between the maximum load and the bonded area, was used. Furthermore, specimens cleaned only with acetone were made and tested for comparison.

3 Results and discussion

3.1 Effect of laser surface texturing on JBS

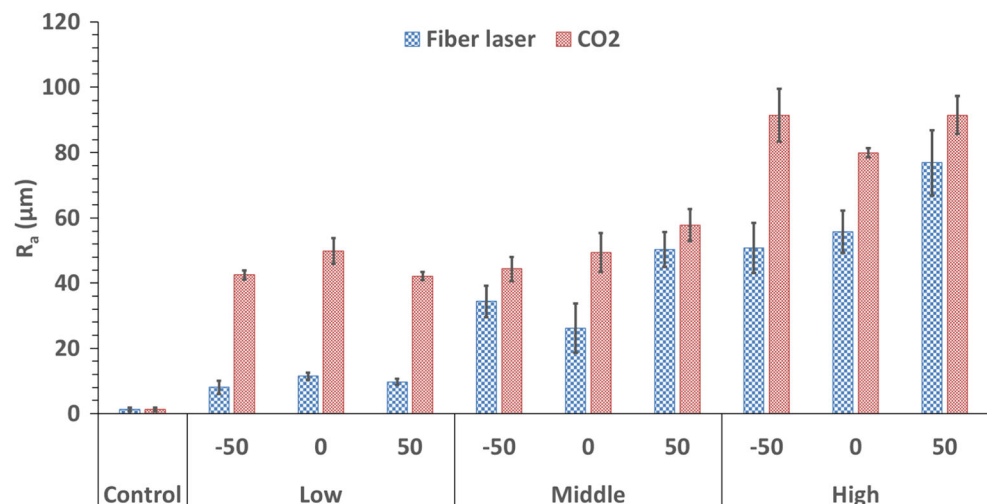
Figures 5 and 6 show the results of the lap shear tests of adhesive bonded joints. The standard deviation of the samples tested is also represented as error bars. The specimens, which were subjected to fiber laser pre-treatment (Fig. 5), show an improvement of the JBS compared to control ones. All laser-treated samples present a substantial reduction in the variability of the results. At higher power levels (500 W and 550 W),

10 mm overlapping joints have JBS values that are very similar to those of 15 mm overlap, if we consider the range of the standard deviation. In addition, the largest increments are noted for the joints made with only 5 mm of overlap, confirming the fact that the surface treatment allows less limiting geometrical configuration (Table 2).

Very good bond strengths were also achieved using the CO₂ laser source (Fig. 6), especially for higher overlaps and even at low power values. For example, with 300 W, at –50% (i.e. with 10 mm overlap) the same JBS was produced as with 15 mm overlap for the control samples. Large increments in JBS were reached at all levels (Table 3), up to a maximum of +63% for 300 W, at 50% overlap (i.e. with 5 mm overlap).

Significant increases in mechanical performance of laser pre-treated adhesive bonded joints were also found on other metal substrates [12, 17] and other geometric configurations [24], in agreement with the results obtained in this study. The explanation of what emerged is mainly attributable to the

Fig. 8 Surface roughness measurements, in terms of R_a



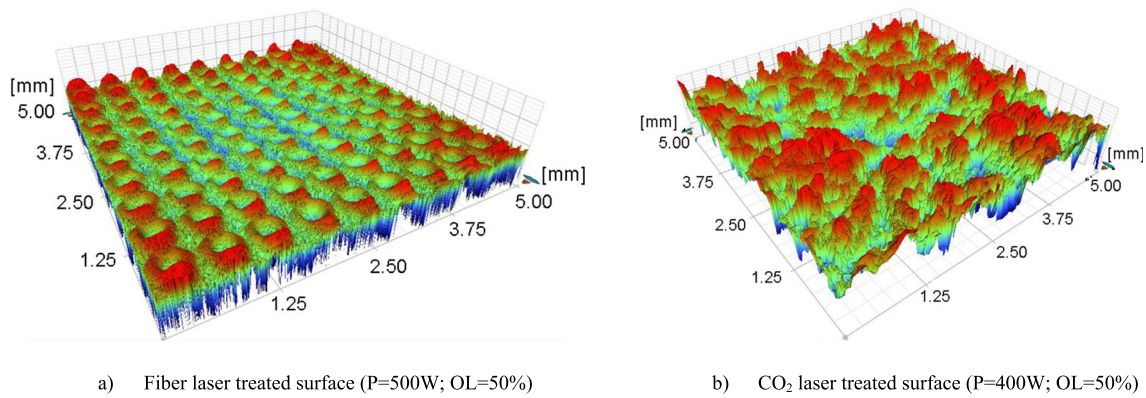


Fig. 9 Morphology evaluation of laser treated surfaces produced by the (a) fiber and (b) CO₂ laser systems

change in surface morphology and is discussed and illustrated further in the next section.

A cohesive failure was detected in all the laser treated samples, both using fiber or CO₂ laser. An example of macro morphology of the fracture failure interfaces of the adhesively bonded joints after tensile tests are displayed in Fig. 7.

3.2 Effect of laser surface texturing on surface morphology

In the context of adhesive bonding, increasing the surface roughness is considered to be a particularly effective method to create the right surface conditions. It is in fact connected to an increase of the area on which the adhesive bonds can actually be made and allows the creation of a mechanical interlocking [25]. In this work, the effect on the surface morphology of two different laser sources is studied and compared.

The bar graph shown in Fig. 8 indicates the effectiveness of both the laser treatments compared to the control sample. In particular, the CO₂ laser substantially modified the surface roughness, especially at the highest level of power.

For the fiber laser, the ablation at lower values exhibited a limited effect on the surface roughness. This value increases

moving to middle and high values of laser power (500 W and 550 W), following the increase of JBS values. Interestingly, several treatments exhibit similar surface roughness measurements using the different laser sources, but the actual morphology is significantly different, as shown in Fig. 9.

Similar results were obtained on the same material by Obeidi et al., in which the high levels of irradiance and residence time exhibited comparable values and a wide range of roughness. This effect can be explained by the fact that larger melt pool sizes result in molten material jetting and spreading [21].

The link between the value of R_a and recorded tensile shear strength (TSS) is represented in Fig. 10. It is worth noting that the fiber laser creates morphology with roughness values in a much wider range and the trends of the TSS values are divergent for the two sources. In particular, the values of TSS show a decreasing trend with increasing R_a if the samples are prepared with a CO₂ laser, while they increase if prepared with a fiber laser.

This behavior is probably due to the different surface morphology generated (Fig. 11). Peaks and valleys generated by the fiber laser treatment have a more regular trend and allow better insertion of the adhesive, even for high power values. With regard to the CO₂ laser, generating a surface structure of

Fig. 10 Tensile shear strength (TSS) of the resulting joint versus the prepared surface roughness levels

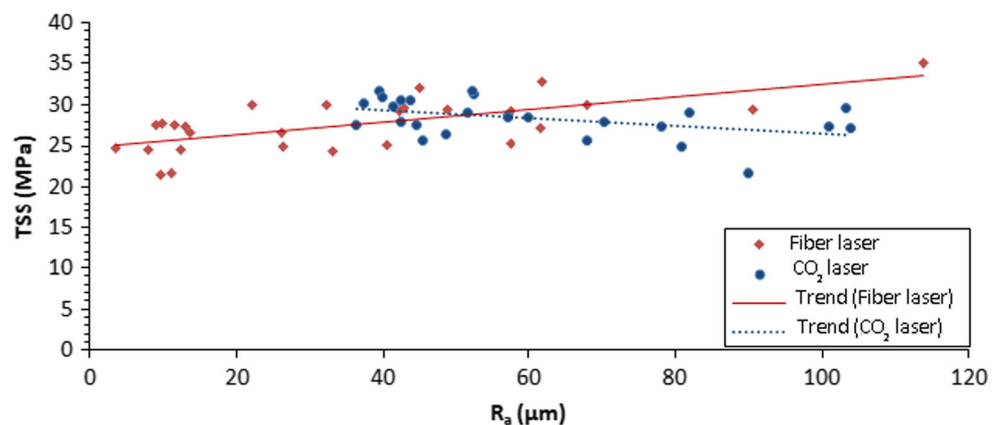


Fig. 11 Surface morphology generated by middle value of laser power, using (a) fiber and (b) CO₂ laser systems



less marked roughness is preferable, permitting a correct inclusion of the adhesive between the peaks and valleys of the surface and avoiding a peak-to-peak contact.

3.3 Statistical analysis

The results of the study were statistically analyzed to understand the significance of the main parameters and to generate predictive models of adhesive-joint behavior.

The results exhibit significant correlations in the model between the input parameters, the output measures, and the joint bond strength. The solver employed was quadratic in which the p value was less than 0.0001 as an indication of this correlation significance. Moreover, the adjusted R^2 value for the solver was 0.9878 for the fiber laser process and 0.9727 for the CO₂ process, which means that the data fit the regression line well. Similarly, the two models can predict 97.79% (fiber laser) and 96.42% (CO₂ laser) of an untested value within the examined range of the processing parameters according to the predicted R^2 value.

In particular, Fig. 12 shows the actual data plotted versus the predicted data for the analysis of both laser sources. All data are close and well distributed around the neutral line.

The statistical analysis can be found in Table 4. Each p value can be found in this table, in which the correlation between the corresponding factors is indicated.

From Fig. 5, it can be seen that the joint overlap has the most significant effect on the joint bond strength with some improvement in the low power level compared to the control set of joints. Higher (JBS) were obtained in the samples textured by the CO₂ laser shown in Fig. 6. In this figure, the set processed with the low power level also exhibits the higher JBS contributed to the lower surface roughness, see Fig. 7.

The reduction in the JBS with the increase in the surface roughness is likely due to the difficulty for the adhesive material to reach the lower valleys of these rougher surfaces, thereby leaving air pockets between the metal surface and the adhesion. This would lead to a reduction of the total surface area engaged with chemical bonding.

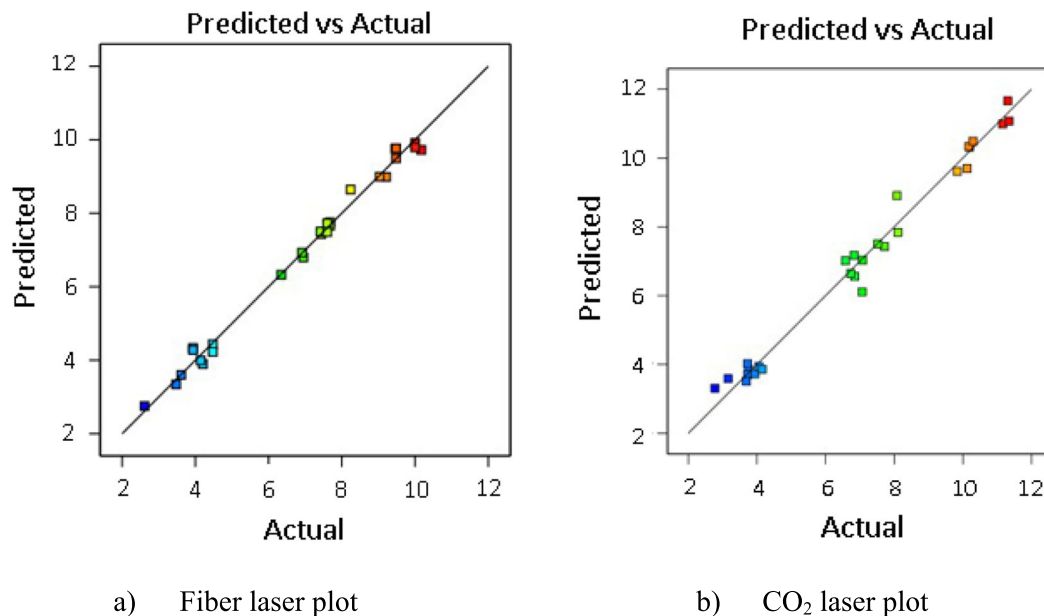


Fig. 12 Actual data versus predicted data plots

Table 4 ANOVA responses for different laser sources on JBS

Source	Sum of square	<i>df</i>	Mean square	<i>F</i> value	<i>P</i> value
Fiber laser					
Model	148.48	9	16.50	235.63	< 0.0001
A—Laser power	3.40	1	3.40	48.55	< 0.0001
B—Pulse overlap	0.3819	1	0.3819	5.45	0.0320
C—Joint overlap	140.05	1	140.05	2000.27	< 0.0001
AB	0.2812	1	0.2812	4.02	0.0613
AC	0.0126	1	0.0126	0.1801	0.6766
BC	0.1860	1	0.1860	2.66	0.1215
A ²	1.63	1	1.63	23.29	0.0002
B ²	0.1680	1	0.1680	2.40	0.1398
C ²	2.37	1	2.37	33.81	< 0.0001
Residual	1.19	17	0.0700		
Cor total	149.67	26			
CO₂ laser					
Model	205.31	6	34.2	199.48	< 0.0001
A—Laser power	4.05	1	4.05	23.60	< 0.0001
B—Pulse overlap	1.47	1	1.47	8.57	0.0083
C—Joint overlap	66.94	1	66.94	390.22	< 0.0001
AB	0.0431	1	0.0431	0.2511	0.6217
AC	0.8003	1	0.8003	4.67	0.0431
BC	0.7620	1	0.7620	4.44	0.0479
Residual	3.43	20	0.1715		
Cor total	208.74	26			

Figure 13 show the response surface method (RSM) graphs, which explain the correlation between two input processing parameters and the output measures in one value of

the third parameter in 3D view. The variation in the JBS values is directly proportional to the joint overlap in both laser system texture. There is noticeable enhancement in the JBS

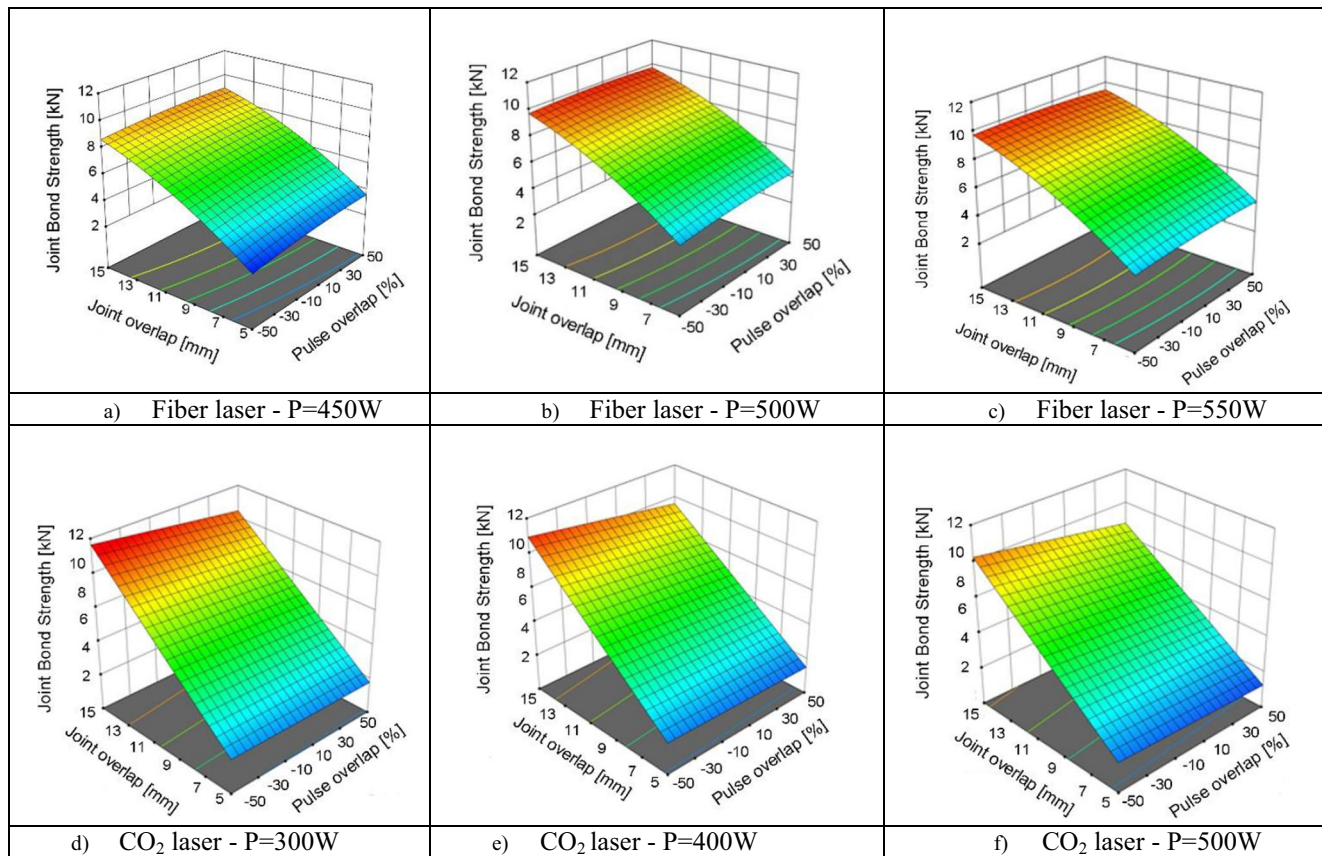


Fig. 13 Response surfaces indicating the effects of joint overlap and pulse overlap on the joint bond strength at different power levels

with the increase of the surface roughness in the lower laser power level compared to the control (un-textured) samples due to the increase of the surface area and the specific area. This strength is reduced with the further increase in surface roughness for the aforementioned reason.

4 Conclusion

The laser surface texturing process was used to create defined surface morphologies and increase joint bond strength.

Two sources, a fiber laser and a CO₂ laser, were used for surface modification. Laser power, pulse overlap, and joint overlap were the varied process input parameters and surface profile and bond strength were the recorded outputs. The conclusions are summarized as follows:

- A significantly increase was achieved in joint bond strength using both laser sources. Within the laser parameter range investigated, smaller joint surface overlaps could be implemented to achieve bond strengths of similar magnitude to that from much larger overlaps when using the non-textured surfaces;

- Surface morphology and the consequent average surface roughness were evaluated, and peak and valley geometries were linked to the laser process parameters. This surface texturing significantly effects the level of surface roughness generated and can be controlled. It is indeed possible to generate surface morphologies able to increase the efficiency of the mechanical interlocking effect.

- A statistical analysis was carried out using response surface methodology to relate the JBS with the process parameters. The variations in the JBS values were directly proportional to the joint overlap for the laser textures prepared with both laser systems.

- Although the creation of the model is linked to the specific adhesive system and process parameters, the method applied provides guidance for process mapping with similar systems and applications. Further studies could thereby extend this work to other process parameter ranges and to other substrate materials, adhesives and laser sources. Hence, this work, presents a robust methodology to maximize the effect of laser treatment to achieve the highest levels of adhesive bond strength.

Acknowledgements The authors gratefully acknowledge Chiara De Giorgi and IPG Photonics Italy S.r.l for the support provided in fiber laser surface treatment. The authors wish also to thank 3M Italy for the constant support in carrying out research activities on adhesive bonding technology.

Funding information This work was part funded from research supported by a research grant from Science Foundation Ireland (SFI) under grant number 16/RC/3872 and is co-funded under the European Regional Development Fund.

References

1. Baldan A (2004) Review adhesively-bonded joints and repairs in metallic alloys, polymers and composite materials: adhesives, adhesion theories and surface pretreatment. *J Mater Sci* 39:1–49
2. Van Dam JPB, Abrahams ST, Yilmaz A et al (2019) Effect of surface roughness and chemistry on the adhesion and durability of a steel-epoxy adhesive interface. *Int J Adhes Adhes* 96: 102450. <https://doi.org/10.1016/j.ijadhadh.2019.102450>
3. Brack N, Rider AN (2014) The influence of mechanical and chemical treatments on the environmental resistance of epoxy adhesive bonds to titanium. *Int J Adhes Adhes* 48:20–27. <https://doi.org/10.1016/j.ijadhadh.2013.09.012>
4. Cardoso JV, Gamboa PV, Silva AP (2019) Effect of surface pretreatment on the behaviour of adhesively-bonded CFRP T-joints. *Eng Fail Anal* 104:1188–1202. <https://doi.org/10.1016/j.engfailanal.2019.05.043>
5. Prysiaznyh V, Svoboda T, Dvořák M, Klíma M (2012) Aluminum surface treatment by the RF plasma pencil. *Surf Coatings Technol* 206:4140–4145. <https://doi.org/10.1016/j.surfcoat.2012.04.010>
6. Mandolfino C, Lertora E, Gambaro C, Pizzorni M (2019) Functionalization of neutral polypropylene by using low pressure plasma treatment: effects on surface characteristics and adhesion properties. *Polymers (Basel)* 11. <https://doi.org/10.3390/polym11020202>
7. Bizibandoki P, Benayoun S, Valette S et al (2011) Modifications of roughness and wettability properties of metals induced by femtosecond laser treatment. *Appl Surf Sci* 257:5213–5218. <https://doi.org/10.1016/j.apsusc.2010.12.089>
8. Alloys A, Treatment CA (2000) Standard guide for preparation of metal surfaces for adhesive bonding 1. *Society* 90:1–6. <https://doi.org/10.1520/D2651-01R08.2>
9. Grabowski A, Sozańska M, Adamiak M, Kepińska M, Florian T (2018) Laser surface texturing of Ti6Al4V alloy, stainless steel and aluminium silicon alloy. *Appl Surf Sci* 461:117–123. <https://doi.org/10.1016/j.apsusc.2018.06.060>
10. Kurtovic A, Brandl E, Mertens T, Maier HJ (2013) Laser induced surface nano-structuring of Ti-6Al-4V for adhesive bonding. *Int J Adhes Adhes* 45:112–117. <https://doi.org/10.1016/j.ijadhadh.2013.05.004>
11. Lunder O, Lapique F, Johnsen B, Nisancioglu K (2004) Effect of pre-treatment on the durability of epoxy-bonded AA6060 aluminium joints. *Int J Adhes Adhes* 24:107–117. <https://doi.org/10.1016/j.ijadhadh.2003.07.002>
12. Loutas TH, Kliafa PM, Sotiriadis G, Kostopoulos V (2019) Investigation of the effect of green laser pre-treatment of aluminum alloys through a design-of-experiments approach. *Surf Coatings Technol* 375:370–382. <https://doi.org/10.1016/j.surfcoat.2019.07.044>
13. Moroni F, Romoli L, Khan MMA (2018) Design of laser-textured surfaces to enhance the strength of adhesively bonded joints. *Int J Adhes Adhes* 85:208–218. <https://doi.org/10.1016/j.ijadhadh.2018.06.001>
14. Musiari F, Moroni F, Favi C, Pironi A (2019) Durability assessment of laser treated aluminium bonded joints. *Int J Adhes Adhes* 93:102323. <https://doi.org/10.1016/j.ijadhadh.2019.01.017>
15. Rechner R, Jansen I, Beyer E (2010) Influence on the strength and aging resistance of aluminium joints by laser pre-treatment and surface modification. *Int J Adhes Adhes* 30:595–601. <https://doi.org/10.1016/j.ijadhadh.2010.05.009>
16. Juan YC, Song MX, Ling TY et al (2016) Modification of wettability property of titanium by laser texturing. *Int J Adv Manuf Technol* 87:1663–1670. <https://doi.org/10.1007/s00170-016-8601-9>

17. Wu Y, Lin J, Carlson BE, Lu P, Balogh MP, Irish NP, Mei Y (2016) Effect of laser ablation surface treatment on performance of adhesive-bonded aluminum alloys. *Surf Coatings Technol* 304: 340–347. <https://doi.org/10.1016/j.surfcoat.2016.04.051>
18. Rotella G, Orazi L, Alfano M, Candamano S, Gnilitzky I (2017) Innovative high-speed femtosecond laser nano-patterning for improved adhesive bonding of Ti6Al4V titanium alloy. *CIRP J Manuf Sci Technol* 18:101–106. <https://doi.org/10.1016/j.cirpj.2016.10.003>
19. Rotella G, Alfano M, Schiefer T, Jansen I (2015) Enhancement of static strength and long term durability of steel/epoxy joints through a fiber laser surface pre-treatment. *Int J Adhes Adhes* 63:87–95. <https://doi.org/10.1016/j.ijadhadh.2015.08.009>
20. Ahmed Obeidi M, McCarthy E, Brabazon D (2016) Methodology of laser processing for precise control of surface micro-topology. *Surf Coatings Technol* 307:702–712. <https://doi.org/10.1016/j.surfcoat.2016.09.075>
21. Obeidi MA, McCarthy E, Kailas L, Brabazon D (2018) Laser surface texturing of stainless steel 316L cylindrical pins for interference fit applications. *J Mater Process Technol* 252:58–68. <https://doi.org/10.1016/j.jmatprotec.2017.09.016>
22. ISO (1997) ISO 4287:1997 Geometrical Product Specifications (GPS)—surface texture: profile method—terms, definitions and surface texture parameters
23. ASTM D 1002–05 (2005) Standard test method for apparent shear strength of single-lap-joint adhesively bonded metal specimens by tension loading (metal-to-metal). Standards 1–5. <https://doi.org/10.1520/D1002-10.on>
24. Romoli L, Moroni F, Khan MMA (2017) A study on the influence of surface laser texturing on the adhesive strength of bonded joints in aluminium alloys. *CIRP Ann - Manuf Technol* 66:237–240. <https://doi.org/10.1016/j.cirp.2017.04.123>
25. Wegman RF, Van Twisk J, Wegman RF, Van Twisk J (2013) Introduction. In: *Surface preparation techniques for adhesive bonding*. Elsevier, pp 1–8

Publisher's note Springer Nature remains neutral with regard to jurisdictional claims in published maps and institutional affiliations.